Journal of NeuroVirology (2026) 32:35
https://doi.org/10.1007/s13365-026-01337-3

RESEARCH

SARS-CoV-2 disrupts the integrity of a human blood-brain barrier model in the absence of infection

Habib Jmii[1] · Ruth Haverty[1] · Keith D Rochfort[2] · Nicola F Fletcher[1]

Received: 30 January 2026 / Revised: 27 July 2026 / Accepted: 12 August 2026

Abstract

Neurological symptoms are recognized in patients with COVID-19, and include anosmia, ageusia, cognitive impairments as well as more severe complications including encephalitis and ischemic strokes. Furthermore, persistent cognitive impairment including 'brain fog' is recognised as part of the long COVID syndrome. While SARS-CoV-2 has been shown to infect cells of the central nervous system (CNS) in vitro and in vivo, it is unclear whether direct infection of the CNS or indirect mechanisms including activation of the coagulation cascade or immune activation are the key drivers of COVID-19 neuropathology. We investigated whether inactivated SARS-CoV-2, or spike protein, can disrupt the integrity of the blood-brain barrier (BBB) and characterised neuroinflammation in the absence of infection. Using an in vitro model of the BBB composed of primary human microvascular endothelial cells, astrocytes, pericytes and microglia, we observed BBB disruption following exposure of the model to SARS-CoV-2 or spike protein. Importantly, loss of BBB integrity was observed in response to luminal (mimicking 'blood side') or abluminal ('brain side') exposure to inactivated virus or spike protein. Transcriptional upregulation of a range of chemokines, inflammatory cytokines and adhesion factors, and release of inflammatory cytokines from BBB models was also observed in response to luminal or abluminal SARS-CoV-2 or spike protein exposure. These data indicate that BBB disruption and immune activation in vitro occurs in response to SARS-CoV-2 in the absence of infection, highlighting the importance of the host immune system in BBB disruption during SARS-CoV-2 infection.

Keywords Immunopathology · Neuropathology · Neuroinflammation · Microvascular endothelium · Neurovascular unit

Introduction

Multiple clinical reports have highlighted the association between SARS-CoV-2 infection and central nervous system (CNS) disorders with varying degrees of severity ranging from headache to more severe complications including encephalitis, ischemic strokes, and vascular events (Helms et al. 2020; Mao et al. 2020; Nuzzo et al. 2021). The presence of SARS-CoV-2 in the CNS has been demonstrated through the detection of SARS-CoV-2 RNA in the cerebrospinal fluid of infected patients, and in post-mortem brain tissue from patients with COVID-19, indicating that SARS-CoV-2 can infect the central nervous system (Ramani et al. 2020; Song et al. 2021; Wang et al. 2020). The route by which SARS-CoV-2 enters the CNS is incompletely understood. Initially, it was reported that SARS-CoV-2 travels along the olfactory nerves (or other nerve tracts) to the brain (Aragao et al. 2020; Briguglio et al. 2020; Meinhardt et al. 2021) but subsequent studies have suggested that SARS-CoV-2 invasion of the CNS also occurs via the hematogenous pathway after overcoming the blood-cerebrospinal fluid barrier (Fuchs et al. 2021; Pellegrini et al. 2020; Yang et al. 2021) or the blood-brain barrier (BBB) (Krasemann et al. 2022; Rodriguez-Morales et al. 2022; Zhang et al. 2021). Furthermore, indirect mechanisms via virus-induced activation of the immune response or endothelial damage via activation of the coagulation cascade or a 'cytokine storm' have been proposed as the cause of neurological symptoms in COVID-19 patients, and it is possible that either or combined mechanisms may play a role in the pathogenesis of SARS-CoV-2 neurological disease (Pang et al. 2024).

✉ Nicola F Fletcher
Nicola.fletcher@ucd.ie

[1] School of Veterinary Medicine, Conway Institute of Biomedical and Biomolecular Research, University College Dublin, Belfield, Dublin Dublin 4, Ireland

[2] School of Biotechnology and Life Sciences Institute, Dublin City University, Dublin, Ireland

Published online: 26 August 2026

The BBB is a component of the neurovascular unit (NVU) and acts as the blood-brain interface, mediating communication between the CNS and the periphery (Rhea and Banks 2019). In addition, the BBB is a major barrier that restricts the passage of pathogens, including viruses or virus-infected cells, into the brain parenchyma. The BBB is formed by brain microvascular endothelial cells (BMECs), supported by pericytes, astrocytes, microglia, basement membrane, and neurons (Naranjo et al. 2022). A core property of BMEC is the strict regulation of paracellular permeability due to junctional complexes (tight [TJ], adherens [AJ], and gap junctions [GJ]) between endothelial cells that limit passive diffusion (Pong et al. 2020). However, many pathogens can circumvent the BBB and enter the brain, including human immunodeficiency virus (Osborne et al. 2020) and flaviviruses including West Nile virus (Roe et al. 2012, 2014). BBB disruption and dysfunction prompts the leakage of blood constituents into the CNS, infiltration of various cells, abnormal transfer and clearance of ions and molecules responsible for reduction and dysregulation of cerebral blood flow causing various neurological disorders (Alajangi et al. 2022). Several studies have investigated the interaction between SARS-CoV-2 and the BBB using in vitro models or BBB organoids (Constant et al. 2021; Krasemann et al. 2022; Nascimento Conde et al. 2020; Wenzel et al. 2021; Yang et al. 2021; Zhang et al. 2021). However, many questions remain unanswered regarding our understanding of the interaction between SARS-CoV-2 and the BBB. The ability of SARS-CoV-2 to directly infect the BBB, the effect of viral infection on BBB integrity, the mechanism by which SARS-CoV-2 may cross the BBB, and the role of the inflammatory response in BBB disruption, is incompletely understood.

In the present study, we investigated the effect of SARS-CoV-2 to disrupt the BBB, and characterized the inflammatory response to spike protein or full-length virus, in the absence of infection. We generated an in vitro BBB model composed of a quadruple co-culture of primary human BMECs, astrocytes, pericytes, and microglia that recapitulates many features of the BBB. Using recombinant SARS-CoV-2 spike protein or heat inactivated SARS-CoV-2, we investigated the ability of SARS-CoV-2 to disrupt BBB integrity and induce proinflammatory responses at the BBB.

Methods

Cells and viruses

Primary human brain microvascular endothelial cells (BMEC)(Cell Systems ACBRI-376), primary astrocytes (ScienCell #1800), human brain vascular pericytes (ScienCell #1200), and microglia (ScienCell #1900) were grown in specialized medium (endothelial cell medium (Cell Systems 4ZO-500); astrocyte medium (ScienCell #1801), pericyte medium (ScienCell #1201), and microglia medium (ScienCell #1901), respectively, according to the manufacturers' instructions. To promote cell adherence, flasks were precoated with attachment factor (Cell Systems, 4Z0-210) for BMEC, poly-L-Lysine (Sigma-Aldrich, P4832) for astrocytes and pericytes, and type I bovine collagen (Corning, 354231) for microglia. SARS-CoV-2 (2019-nCoV/Italy-INMI1 strain from EVA Global) was propagated in VeroE6 cells as previously described (Haverty et al. 2024). Briefly, VeroE6 cells (ATCC), cultured in Dulbecco's modified Eagle medium (DMEM) supplemented with 10% foetal bovine serum (FBS), were used for virus amplification and titration by TCID50 assay. All virus used in this study was at passage 3. Cells were inoculated with an MOI of 0.01 for 2 h, washed with phosphate buffered saline (PBS), and the medium replaced with DMEM containing 2% FBS. When cultures exhibited greater than 90% cytopathic effect (CPE), flasks were freeze-thawed three times and supernatants collected and clarified at 3500 r.p.m. for 30 min at 4 °C. Virus-containing supernatant was aliquoted and stored at −80 °C. TCID50 was determined in VeroE6 cells in quadruplicate and infectious titre was determined using the Reed-Muench method prior to heat inactivation by incubation at 56 °C for 30 min. Complete inactivation of virus was confirmed by TCID50 assay.

Establishment of in vitro human BBB model

The quadruple cell in vitro BBB model was established as described (Stone et al. 2019) with minor modifications. Transwell inserts (Corning, Catalogue number 3460) were inverted and the basolateral side was coated with poly-L-lysine for 1 h. Primary human astrocytes (3×10^5 cells) were seeded on the basolateral side of the inserts and allowed to adhere for 1 h at 37 °C, then the inserts were inverted into a 12-well plate and incubated overnight in astrocyte medium. The following day, pericytes (6.25×10^4 cells) were added to the astrocyte cell layer on the basolateral side of the inserts and incubated at 37 °C. After 2 hours, excess pericyte medium was aspirated from the basolateral side of the inserts, inserts were inverted and placed in a 12-well plate, and a 1:1 mixture of astrocyte and pericyte medium was added to the apical and basolateral compartments. Once astrocytes and pericytes reached confluency (assessed using visual inspection by light microscopy), medium in the apical compartment was aspirated, the membrane was coated with attachment factor (Cell Systems) and BMEC (7.5×10^4 cells) were seeded on the apical compartment of the inserts. On the same day, microglia were separately plated in 12-well plates coated with type I bovine collagen, at a density of 2.5×10^4 cells/well and allowed to reach confluence for 4

days. Transwell inserts containing BMEC, astrocyte and pericyte co-cultures were then transferred to 12 well plates containing microglia. Fresh BMEC medium was applied to the apical compartment and a mixture of pericyte, astrocyte and microglial medium (1:1:2) was added to the basolateral compartment. Two days later, the integrity of the BBB models was assessed by measurement of Transendothelial Electrical Resistance (TEER) using STX2 chopstick electrodes connected to an EVOM2 voltmeter (World Precision Instruments). TEER was expressed as $\Omega.cm^2$, with a correction applied to the values obtained from the EVOM2 voltmeter to account for the surface area of the Transwell inserts (1.2 cm^2). The BBB models were used for experiments when they exhibited a TEER value of ≥ 45 $\Omega.cm^2$ greater than Transwell inserts alone (Stone et al. 2019). Alternatively, BBB tight junction integrity was quantified by determination of the permeability of the BBB models to 40 KDa FITC-conjugated dextran (Sigma, FD40S) as previously described, with minor modifications (Harati et al. 2022). Briefly, FD40 was added to the apical chamber of the models at a concentration of 0.25 mg in 500ul of phenol red-free DMEM supplemented with 2% FBS and incubated for 3 h at 37 °C with 5% CO2. Accumulation of FD40 in the basolateral chamber was quantified by measurement of fluorescence intensity using a fluorescence plate reader (Molecular Devices, SpectraMAX Gemini, excitation: 490 nm, emission: 525 nm). Percent permeability was calculated as the relative fluorescence of medium from treated vs. untreated BBB models.

Treatment of BBB models with heat-inactivated SARS-CoV-2 or spike protein

To determine the effect of SARS-CoV-2 on BBB integrity in the absence of viral replication, BBB models were treated via the apical compartment with heat-inactivated SARS-CoV-2 at an equivalent MOI of 1. In addition, different BBB constructs were treated with full-length SARS-CoV-2 spike protein (Sigma, AGX819) at concentrations ranging from 0.5 to 5 µg. A combination of recombinant human IFN-g and TNF-α (100ng each; PeproTech) was used as a positive control for BBB disruption. BBB models mock-inoculated with spent VeroE6 media from uninfected cultures were used as negative controls. At various times post-treatment, ranging from 24 to 72 h, BBB integrity was evaluated by TEER measurement and FD40 permeability assays. We chose 72 h as the optimal timepoint to measure tight junction integrity based on our initial observations that maximal BBB disruption was detected 72 h post exposure to spike and SARS-CoV-2. However, as acute proinflammatory responses to antigen stimuli are rapid (Megha et al. 2021) we chose to quantify responses to spike and SARS-CoV-2 at a shorter time post exposure (24 h).

Quantitative PCR

Following treatment with SARS-CoV-2 spike protein (0.5–5 µg), BMEC RNA was extracted according to the method of Chomczynski and Sacchi (Chomczynski and Sacchi 2006) using TRIzol® reagent (Thermo Fisher Scientific, MA, USA). cDNA was generated from 1 ug of RNA using a high-capacity cDNA reverse transcription kit (Thermo Fisher Scientific, MA, USA). cDNA concentration was determined using a NanoDrop One Spectrophotometer (Thermo Fisher Scientific, MA, USA). Amplification of target cDNA sequences using gene-specific primers (Table 1) was performed by qPCR using a Roche LightCycler® 96 Instrument (Roche Diagnostics, IN, USA). PCR reaction mixtures (25 ul) were as follows: 12.5 ul of FastStart Universal SYBR Green/Rox Mastermix (Roche Diagnostics, IN, USA), 8.5 ul of RNAse/DNAse-free water, 2 ul of cDNA, 1 ul of both 10 µm forward and reverse primer. PCR reaction conditions were as follows: denaturation at 95 °C for 5 min, followed by 40 cycles of (i) denaturation at 95 °C for 15 s, (ii) annealing at 59 °C for 30 s, and (iii) extension at 72 °C for 15 s. Each cDNA sample was assayed in triplicate and results were prepared using the ΔΔCq method. Glyceraldehyde phosphate dehydrogenase (GAPDH) was used for normalisation purposes following validation of multiple housekeeping genes across different human brain cell types in vitro. This was previously published using the Primer Design geNorm kit with 12 housekeeping genes. All primer pairs were compliant with MIQE guidelines.

Protein harvesting and western blot

Following treatment with SARS-CoV-2 spike protein (0.5-5 ug), BMEC lysates were washed with ice cold phosphate-buffered saline (PBS) before being lysed with the addition of RIPA-SDS lysis buffer supplemented with 1x protease/phosphatase inhibitor cocktail. Lysates were transferred into a pre-chilled microfuge tube and rotated for 1 h at 4 °C.

Table 1 Primer sequences used for quantitative PCR

Gene	Primer Sequence
Claudin-5	Forward gaggcgtgctctacctgttt
	Reverse agtacttcacggggaagctg
ZO-1	Forward gaacgaggcatcatccctaa
	Reverse ccagcttctcgaagaaccac
VE-Cadherin	Forward cagcccaaagtgtgtgagaa
	Reverse cggtcaaactgcccaactt
Occludin	Forward ccttcacccccatctgacta
	Reverse gcaggtgctctttttgaagg
JAM-A	Forward accaccagactcgtttgcta
	Reverse cttgaccttgacctccccat
GAPDH	Forward gagtcaacggatttggtcgt
	Reverse ttgattttggagggatctcg

The lysate was clarified of insoluble material by centrifugation at 13,000 RPM for 20 min at 4 °C and the supernatant aliquoted and stored at -80 °C. Protein concentration was determined by bicinchoninic acid (BCA) assay (Pierce, Cramlington, UK) with bovine serum albumin (BSA) used to generate the standard curve.

Following experimental treatments, BMEC lysates were profiled for proteins of the intercellular junction by Western blotting according to the method of Guinan (Guinan et al. 2013) with minor modifications. Briefly, lysates were resolved by SDS-PAGE under reducing conditions using a Mini-PROTEAN® Tetra Cell and Mini Trans-Blot® Module (Bio-Rad, CA, USA) before the proteins were electroblotted to PVDF membrane overnight at 50 V. Membranes were blocked for 60 min in tris-buffered saline (TBS) containing 5% BSA and 0.1% Tween before being incubated overnight in primary antibody with gentle agitation at 4 °C. Primary antibodies were prepared in TBS containing 1% BSA and 0.1% Tween: 1/1000 anti-Claudin 5 mouse monoclonal IgG (clone 4C3C2, Thermo Fisher Scientific, MA, USA), 1/1000 anti-JAM-A rabbit polyclonal IgG (Thermo Fisher Scientific, MA, USA), 1/1000 anti-Occludin mouse monoclonal IgG (clone OC-3F10, Thermo Fisher Scientific, MA, USA), 1/1000 anti-VE Cadherin rabbit polyclonal IgG (Cell Signalling Technology, MA, USA), 1/1000 anti-ZO-1 rabbit monoclonal IgG (clone D6L1E, Cell Signalling Technology, MA, USA), 1/1000 anti-GAPDH rabbit monoclonal IgG (clone 14C10, Cell Signalling Technology, MA, USA). Membranes were then washed three times in TBS containing 0.1% Tween (TBST) before being incubated for 2 h in secondary antibody with gentle agitation at room temperature. Secondary antibodies (Cell Signalling Technology, MA, USA) were prepared in TBST (with 1% BSA): 1:2000 HRP-conjugated goat anti-rabbit (7074 S), or 1:2000 HRP-conjugated horse anti-mouse (7076 S). Membranes were developed using Immobilon Forte Western HRP substrate (Merck Millipore Ltd., Cork, Ireland) followed by chemiluminescent imaging using a G: BOX CHEMI XRQ Multi Fluorescence and Chemiluminescence Imaging System (Synoptics, Cambridge, UK).

RT2 profiler PCR array

Cells from the BBB model (BMECs, astrocytes/pericytes, and microglia) were harvested by manual removal from inserts or culture plates using a cell scraper, and total RNA was extracted with an RNEasy MiniKit (Qiagen) according to the manufacturer's instructions. 200ng of RNA was used for cDNA synthesis using the QuantiTect Reverse Transcription Kit (Qiagen). The expression of genes involved in the anti-viral immune response, cell death, adhesion and tight junction proteins expression and angiogenesis was determined by custom RT² Profiler PCR Array kit (Qiagen). Results were analyzed on Qiagen's web based GeneGlobe design and analysis hub (https://geneglobe.qiagen.com/us/analyze). Gene expression was normalized to the expression of the housekeeping gene GAPDH, according to the manufacturer's instructions.

Quantification of inflammatory cytokines by ELISA

Quantification of cytokines in cell culture medium collected from the apical and the basolateral compartments of the in vitro BBBs was performed using commercial ELISA kits according to the manufacturer's instructions. We determined the concentration of pro-inflammatory cytokines TNF-α (Invitrogen, KHC3011), IL-1β (Invitrogen, KAC1211), IFN-α (Invitrogen, BMS216) and the chemokines CXCL10 (Invitrogen, KAC2361) and MCP1 (Invitrogen, BMS281).

Statistical analysis

Statistical analyses were performed with GraphPad Prism 7 (GraphPad Software, La Jolla, CA, USA). Two-tailed Student's t-test or ANOVA Tukey's test were used to control test groups to control group or for multiple comparison respectively. Statistical significance was defined by P-values less than 0.05. P-value < 0.05: *, < 0.01: **, < 0.001: ***, < 0.0001: ****.

Results

SARS-CoV-2 and recombinant spike protein compromise BBB integrity

The integrity of the BBB models was assessed at different timepoints post-treatment with SARS-CoV-2 or spike protein by measuring the TEER and permeability to FD40. inoculation with heat-inactivated virus or SARS-CoV-2 spike protein resulted in a reduction of TEER values in a dose and time-dependent manner. TEER values decreased from 50 Ω.cm^2 at the time of inoculation to 26.5 Ω.cm^2 72 h post-treatment with 5 µg of spike protein (Fig. 1B and C). As expected, treatment with IFN-γ and TNF-α led to a significant decrease in TEER values whereas no significant change in mock-inoculated BBB constructs was observed (Fig. 1B). Similarly, TEER values decreased over time post-inoculation with inactivated virus, especially when virus was inoculated on the apical side of the BBB constructs. TEER values decreased from a mean value of 80.88 Ω.cm^2 at the time of inoculation to 39.44 Ω.cm^2 at 72 h post-inoculation (Fig. 1D). Inoculation with heat-inactivated virus at an equivalent MOI of 1 did not result in a decrease in BBB integrity, however treatment with the inflammatory cytokines TNF-α

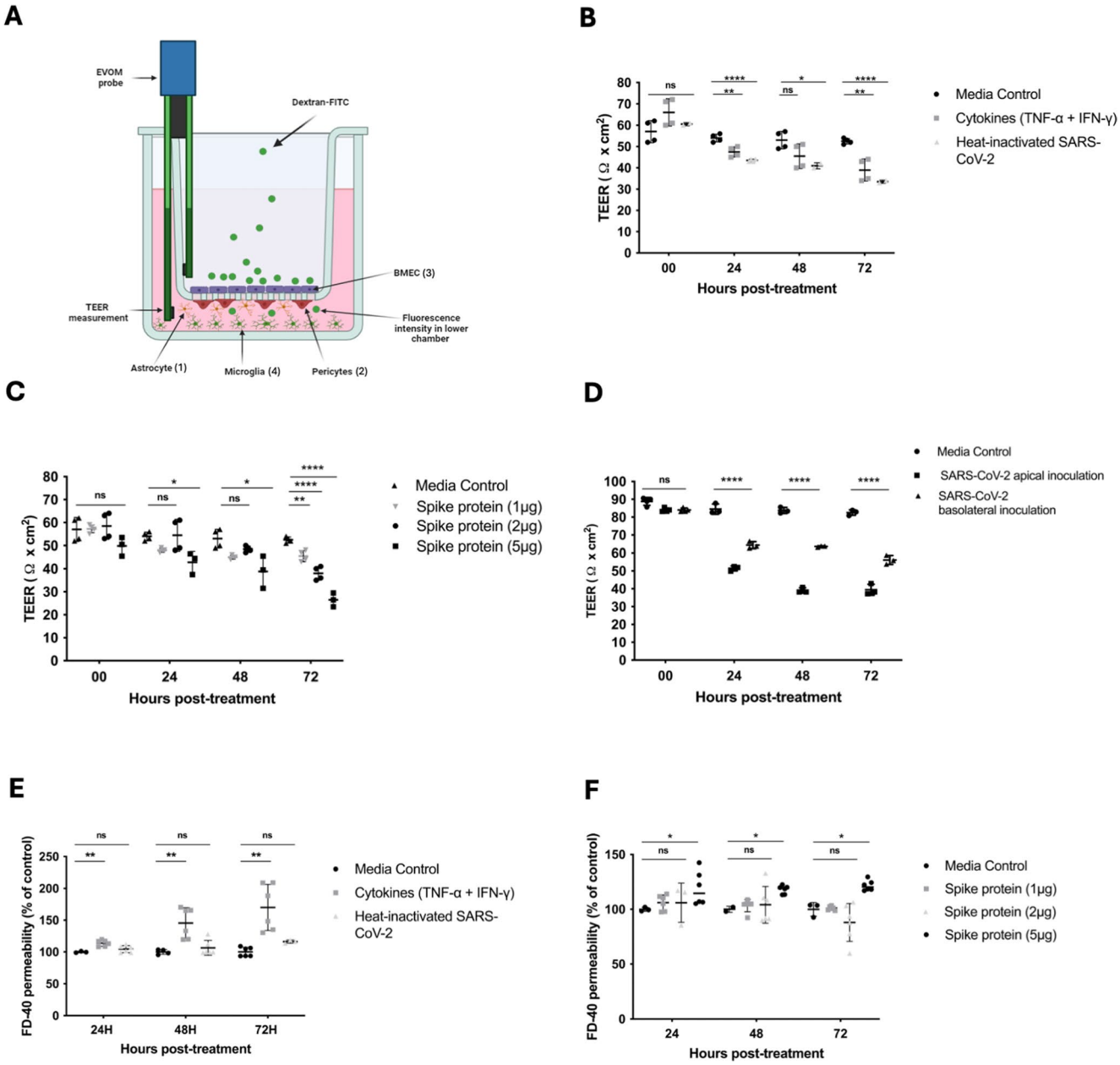

Fig. 1 Figure 1. SARS-CoV-2 and spike protein compromises in vitro BBB integrity. (**A**) Illustration of the in vitro BBB model and the assays carried out to assess BBB integrity. Astrocytes were seeded on the abluminal side of Transwell inserts (1), followed by pericytes (2), brain endothelial cells (3) and inserts were then transferred into culture plates containing microglia (4). (**B**) TEER values recorded from heat-inactivated SARS-CoV-2 or cytokine (TNF-α+IFN-γ) treated BBB models. (**C**) TEER values recorded for BBB models treated with recombinant SARS-CoV-2 spike protein. (**D**) TEER values recorded for BBB models inoculated with heat-inactivated SARS-CoV-2. (**E**) BBB permeability to FITC-dextran 40 kDa (FD40) following treatment with heat-inactivated SARS-CoV-2 or cytokines (TNF-α+IFN-γ). (**F**) BBB permeability to FD40 following treatment with SARS-CoV-2 spike protein. Data are presented as mean +/- standard deviation (n=3 independent replicates). P: < 0.05: *, < 0.01: **, < 0.001: ***. ns=not significant

and IFN-γ significantly increased permeability to FD40 in comparison to mock-treated BBB constructs (Fig. 1E). In addition to TEER measurement, similar increases in permeability to FD-40 were observed, with 5 µg spike protein causing significant disruption to the BBB models, but no significant effect of 1–2 µg spike protein on BBB integrity measured by FD-40 permeability assays (Fig. 1F). We confirmed that there was no effect of mixing the various culture medias used for the different cell types or application of attachment factors to Transwell inserts on cell viability using the CellTiter 96 AQueous One Solution Cell Proliferation MTS Assay (Catalogue G3582, Promega, USA) according

to the manufacturer's instructions. No significant effect on cell viability was observed in any cell type due to the application of attachment factors or mixing of the different cell culture medias used in the final BBB model. Furthermore, visual inspection via light microscopy was performed daily during BBB setup and no visual signs of cell death or altered morphology was observed (data not shown).

SARS-CoV-2 spike protein reduces BMEC tight junction protein expression

Tight junction protein expression in BMEC at the transcriptional and the proteomic level was investigated following treatment with SARS-CoV-2 spike protein. Transcript levels of tight junction proteins were reduced following treatment with spike protein in a concentration and time-dependent manner. The lowest mRNA levels were observed for claudin-5, followed by ZO-1, with a decrease of more than 50% of gene expression 72 h post-treatment with 5 µg of spike protein added to the luminal side of the BBB models. To a lesser extent, the expression of occludin, VECAD, and JAM-1 genes were downregulated following spike protein treatment, especially when cells were treated from the luminal side (Fig. 2A, B). To confirm the results obtained by qPCR, we quantified tight junction protein expression by Western blot and the results were in agreement with the qPCR data. A concentration-dependent effect of spike protein treatment was observed for all tight junction protein expression levels, which was particularly evident for ZO-1, and less importantly for the other tight junction proteins, with a reduction in its expression by more than 50% (Fig. 2A, B, C and D). Inoculation of BMECs with spike protein via the luminal side resulted in a more significant decrease in the expression of tight junction proteins than via the basolateral side (Fig. 2A, B, C and D).

Inoculation with SARS-CoV-2 induces transcriptional upregulation of inflammatory cytokines, proteinases, and adhesion molecules in cells of the BBB

To characterize the immune response following viral treatment of the BBB model, and its potential involvement in SARS-CoV-2 neuropathogenesis, we studied the expression of a set of genes coding for cytokines, chemokines, cell death markers, proteinases, and adhesion molecules in the different components of the neurovascular unit, namely BMEC, microglia, and co-cultured astrocytes and pericytes. 24 h post-inoculation with infectious SARS-CoV-2 from either the luminal or the abluminal side of the BBB constructs, gene expression was assessed by custom RT² Profiler PCR Array and normalized to the gene expression of mock-inoculated cells. In BMECs, inoculation with SARS-CoV-2, either from the luminal or the abluminal side of the BBB, resulted in a significant increase in chemokine gene expression, particularly the chemokine CXCL10 (over 10,000 fold) and CCL5 (over 100 fold). Viral inoculation also significantly induced the expression of the inflammatory transcription factor NF-kB along with pro-inflammatory cytokines such as IL-1β, IL-6, and TNFα. BMEC also had increased expression of the cell adhesion molecule ICAM-1 while PECAM-1 and ITGA-4 expression was downregulated following viral inoculation. Interestingly, we observed a significant increase in the gene expression of MMP-9, which degrades extracellular matrix proteins including tight junction proteins. However, inoculation of our BBB constructs with SARS-CoV-2 led to a decrease in the transcripts of ANGP-1, which plays a role in vascular development and angiogenesis (Fig. 3A, B, E and F).

Following inoculation of the BBB models with SARS-CoV-2 via the luminal or abluminal side, a similar gene expression profile to BMEC was observed in microglia, with increased gene expression of chemokines (CXCL10 and CCL2), cytokines (IL-1β, IL-6, and TNF-α), factors implemented in the inflammatory response such as NF-kB and inflammasome forming proteins NLRP3 and NLRC3 and the adhesion molecule ICAM-1 observed. However, there was no increase in IFN-α gene expression (Fig. 3D and H). A similar expression profile was observed in astrocytes and pericytes compared with microglia following exposure to virus from the apical or the basolateral side of BBB constructs. A large increase in CXCL-10 transcripts and to a lesser extent the chemokines CCL5 and CCL2 and the cytokines TNF-α and IL-1β was observed. The expression of genes involved in the inflammatory response such as the transcription factor NF-kB and the interferon-stimulated genes OAS2 and MYD88 was also induced by viral inoculation along with the proteinase MMP-9 and the adhesion molecule ICAM-1 (Fig. 3C and G). Of note, the inoculation of BBB constructs from the apical side stimulated a greater increase in genes involved in the inflammatory immune response (Fig. 3).

Inoculation with SARS-CoV-2 or spike protein stimulates a pro-inflammatory response in the BBB in vitro

Supernatants were collected from the apical and the basolateral side of BBB models, that had been inoculated with SARS-CoV-2 or spike protein (5 µg) via the luminal **(A)** or the abluminal (B) side, were used to quantify the chemokines MCP-1 and IP-10 and cytokines TNFα, IFNα, and IL-1β at the protein level, to investigate whether viral inoculation triggers an acute inflammatory response that causes BBB disruption. When inoculated from the apical side with inactivated

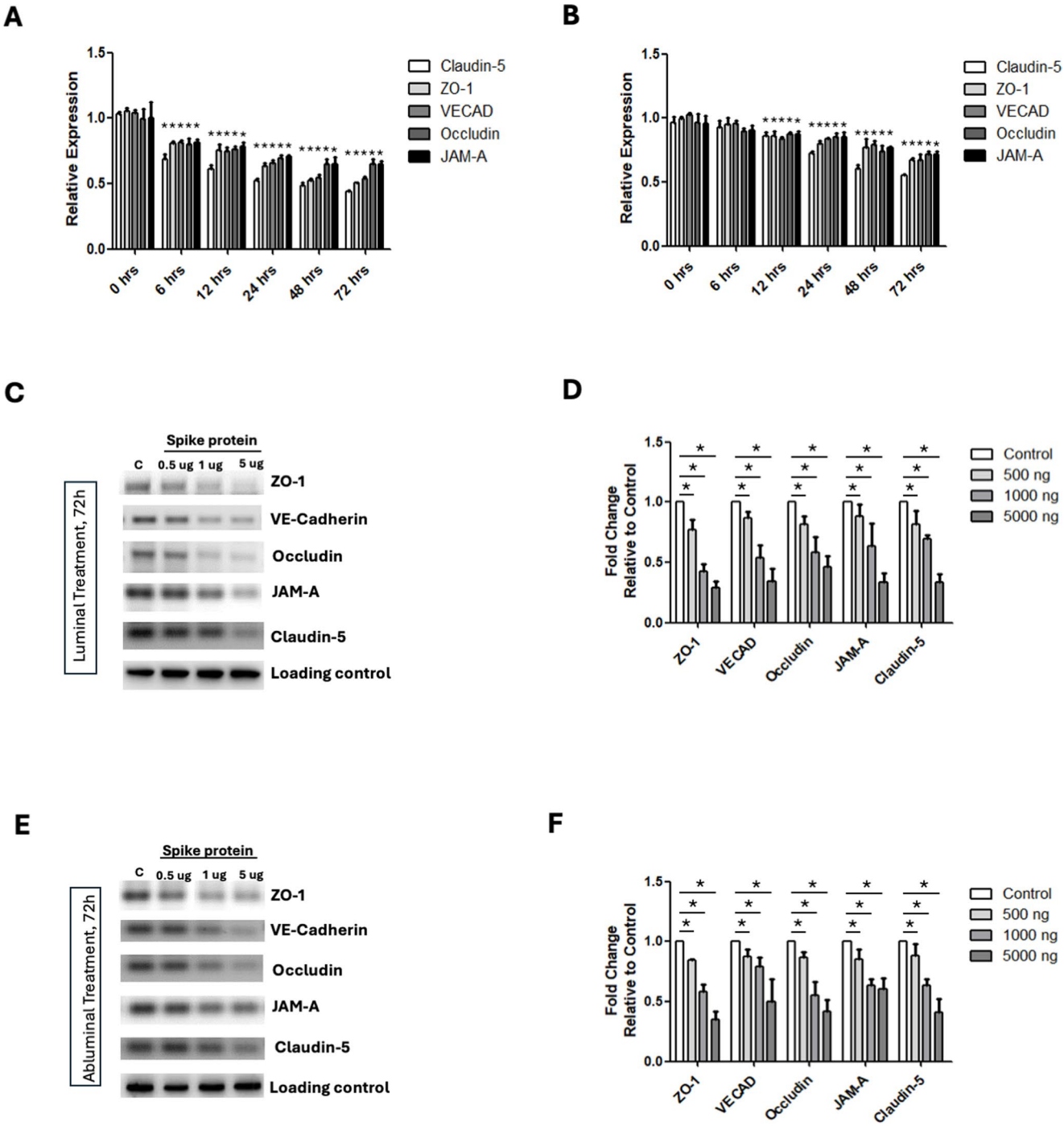

Fig. 2 SARS-CoV-2 spike protein treatment alters the expression of tight junction proteins in BMECs. Expression of tight junction proteins was assessed at the mRNA level (**A**, **B**) as well as the proteomic level (**C**, **D**, **E**, and **F**). mRNA expression of ZO-1, VE-cadherin, occludin, JAM-A and claudin-5 was determined by qPCR at different timepoints post-treatment with 5 µg spike protein from the apical (**A**) or basolateral side (**B**) of BBB constructs. Representative western blot images (**C**, **E**) and summary data (**D**, **F**) of tight junction proteins expression levels in BMECs 72h after the treatment with different concentrations of SARS-CoV-2 spike protein from the luminal (**C**, **D**) or the abluminal side (**E**, **F**) of the BBB models

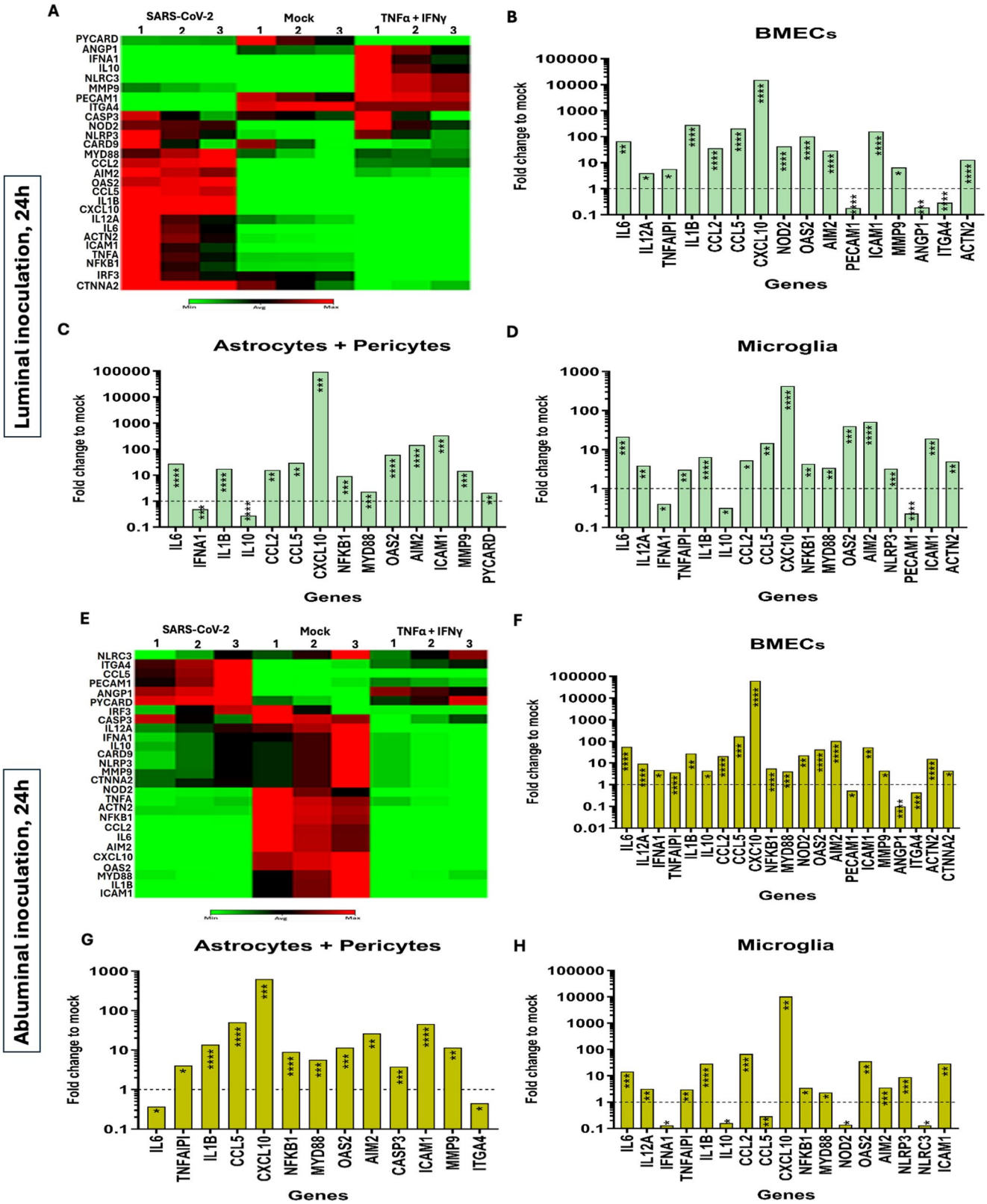
Luminal inoculation, 24h
Abluminal inoculation, 24h
A
SARS-CoV-2
Mock
TNFα + IFNγ
PYCARD
ANGP1
IFNA1
IL10
NLRC3
MMP9
PECAM1
ITGA4
CASP3
NOD2
NLRP3
CARD9
MYD88
CCL2
AIM2
OAS2
CCL5
IL1B
CXCL10
IL12A
IL6
ACTN2
ICAM1
TNFA
NFKB1
IRF3
CTNNA2
B
BMECs
Fold change to mock
Genes
C
Astrocytes + Pericytes
D
Microglia
E
F
G
H

Fig. 3 Inoculation with SARS-CoV-2 induces the expression of inflammatory mediators, adhesion molecules, and proteinases in the BBB model. A. Heatmap of gene expression in BMEC cells in different experimental conditions (Mock, virus-inoculated, and cytokine-treated cells from the luminal side). B, C, and D. Summary plot of significantly regulated genes in BMECs, co-cultured astrocytes and pericytes, and microglia, respectively, 24h post-inoculation with virus from the apical side of the BBB models. E. Heatmap of gene expression in BMECs in different experimental conditions (Mock, virus-inoculated, and cytokine-treated cells from the abluminal side of the BBB constructs). F, G, and H. Summary plot of significantly regulated genes in BMEC cells, co-cultured astrocytes and pericytes, and microglia respectively 24h post-inoculation with the virus from the basolateral side of the BBB models. Data represent the mean values from three independent experiments. Ordinary one-way ANOVA was used to compare treatment groups (SARS-CoV-2 and cytokine-treated BBB models) to the control group (mock-treated BBB models). P: < 0.05: *, < 0.01: **, < 0.001: ***, < 0.0001: ****

SARS-CoV-2 or spike protein, a significant increase in the chemokines MCP-1 and IP-10 was observed, particularly in the luminal compartment, compared to mock-inoculated BBB models (Fig. 4A i and ii). This was also observed for MCP-1 following inoculation with SARS-CoV-2 from the abluminal side which mimics the role of the microglial immune response in BBB disruption following treatment with non-infectious SARS-CoV-2 (Fig. 4B i). IP-10 was not detected following either spike or inactivated SARS-CoV-2 treatment via the basolateral compartment (data not shown). In addition to the chemokines MCP-1 and IP-10, elevated amounts of the major pro-inflammatory cytokine IL-1β was primarily released into the apical compartment following luminal inoculation, and into the basolateral compartment following abluminal inoculation with SARS-CoV-2 (Fig. 4A iii and 4B ii). However, the production of IFN-α did not significantly increase following apical inoculation (Fig. 4A iv) whereas basolateral inoculation caused a significant increase of IFN-α in the apical compartment of the BBB model following SARS-CoV-2 inoculation but not recombinant spike treatment (Fig. 4B iii).

Discussion

Neurological manifestations are common in patients with COVID-19, and include encephalitis, meningitis, dizziness, seizures, ageusia, anosmia and altered consciousness (Aragao et al. 2020; Ermis et al. 2021; Kumar et al. 2020; Mao et al. 2020). These manifestations may also affect other organs, for example SARS-CoV-2 may damage the medullary cardiorespiratory center, which may, in turn, affect respiratory function (Haidar et al. 2022). COVID-19 can also have long-term sequelae such as chronic fatigue, lack of concentration, headache, and depression. Furthermore, it has been suggested that COVID-19 can have a role in of the worsening of neurodegenerative diseases including parkinsonism and Alzheimer's disease (Cavallieri et al. 2022; Reiken et al. 2022). However, the mechanisms by which SARS-CoV-2 causes neuropathology in the CNS are still unclear. Multiple studies have demonstrated that SARS-CoV-2 is capable of infecting cells of the CNS in vitro, including cells of the BBB (Cappelletti et al. 2025; Crunfli et al. 2022; Haverty et al. 2024; Jagst et al. 2024; Proust et al. 2023) and choroid plexus (Pellegrini et al. 2020) as well as animal models (Sia et al. 2020) and humans (Song et al. 2021). Neuropathology has also been proposed to occur following peripheral or central inflammation following SARS-CoV-2 infection (Popa et al. 2025) as well as BBB disruption (Krasemann et al. 2022; Rubin et al. 2025). Viraemia during SARS-CoV-2 is short-lived, however virus may persist in the CNS and exert its effects from the brain side of the BBB. In addition, SARS-CoV-2 endothelial injury and activation, including at the BBB, is associated with a prothrombotic state due to activation of the coagulation cascade and a 'cytokine storm' (de Maistre et al. 2023). However, it remains unclear whether viral infection of the CNS is necessary for COVID-19 associated neurological disease to occur, or if neurological symptoms are driven by inflammatory mechanisms in response to viral antigens.

In the present study, using a multi-cell model composed of primary human brain cells to recapitulate the complex structure of the BBB, we investigated whether BBB disruption and neuroinflammation can occur in the absence of viral replication. Treatment with heat-inactivated SARS-CoV-2 or recombinant spike protein disrupted BBB integrity of the BBB models. Our results are consistent with the majority of published studies that demonstrated the deleterious effect of SARS-CoV-2 on BBB integrity (Buzhdygan et al. 2020; DeOre et al. 2021; Krasemann et al. 2022; Motta et al. 2023; Nascimento Conde et al. 2020; Samudyata et al., 2022; Suprewicz et al. 2022; Yang et al. 2022; Zhang et al. 2021). This observation has been reported by other groups but our study further extended and confirmed these results using a BBB model consisting of primary, differentiated human cells cultured as a multi-cell, physiologically relevant BBB model. Some previous studies have used iPS or organoid models, or cell lines, to investigate SARS-CoV-2 neurological disease in vitro, and in vivo studies using human tissues or human subjects are extremely challenging. We investigated the effects of SARS-CoV-2 on a BBB model composed entirely of primary, differentiated brain cells, rather than cell lines, single primary cell types or iPS cells as have been used in other studies. In contrast, Constant et al. found that SARS-CoV-2 did not alter BBB integrity. The reasons for this are unclear but the study did not use human cells of brain origin, but endothelial cells derived from human umbilical cord blood co-cultured with bovine pericytes (Constant et al. 2021).

We observed increased permeability in our BBB model following inoculation from the luminal or 'blood' side and the abluminal or 'brain' side with the infectious virus or

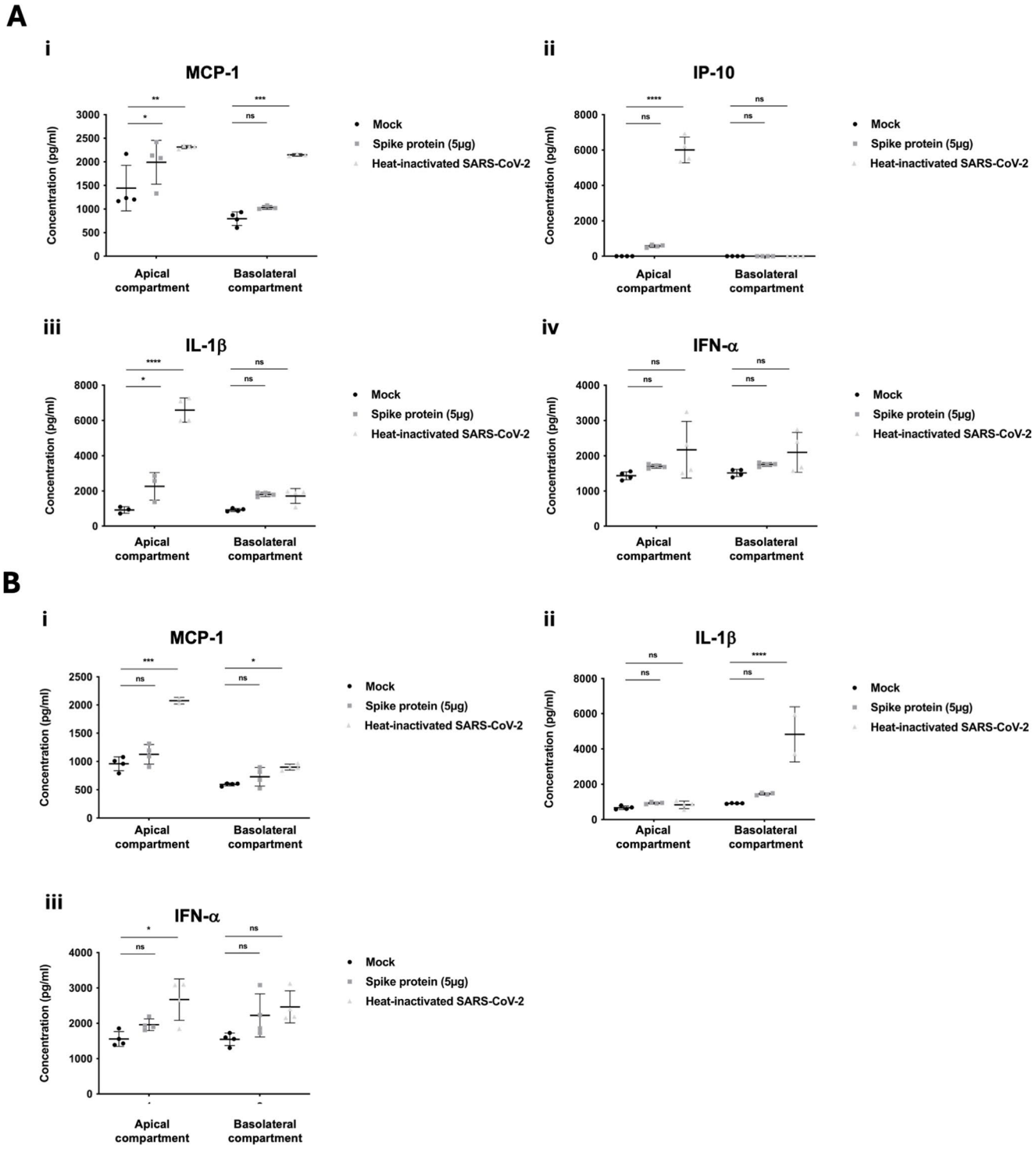

Fig. 4 SARS-CoV-2 or spike protein induces a pro-inflammatory response at the BBB. Cytokine levels in supernatants inoculated via the luminal (**A**) or the abluminal side (**B**) of BBB constructs with SARS-CoV-2, spike protein or mock-inoculated models were assayed from the apical and basolateral compartments 24h post-inoculation. The concentration of chemokines MCP-1 and IP-10 and the cytokines TNF-α, IL-1β and IFN-α were determined by ELISA. Ordinary one-way ANOVA test was used to compare the mean cytokine concentrations released from BBB models (n=4). P: < 0.05: *, < 0.01: **, < 0.001: ***, < 0.0001: ****, P: > 0.05: ns: not significant

spike protein, despite the absence of viral infection of BBB-forming cells. To our knowledge, this is the first report that inactivated SARS-CoV-2 exposure from the abluminal side disrupts BBB integrity. This suggests that the presence of SARS-CoV-2 in the CNS affects the integrity of the BBB, regardless of the route by which the virus gains access to the CNS (neuronal or hematogenous transmission).

We tested whether SARS-CoV-2 might be capable of crossing the BBB via paracellular transport by studying the expression of BMEC tight junction proteins, which form the structural barrier of the BBB and have a crucial role in maintaining BBB integrity and selective permeability (Takata et al. 2021). In our study, despite the lack of productive infection, inoculation with SARS-CoV-2 or spike protein reduced the expression of tight junction proteins at the mRNA and protein levels. Similar findings have been reported in previous studies reporting that SARS-CoV-2 or spike protein disrupts the expression of tight junction proteins suggesting that paracellular transport of SARS-CoV-2 across the BBB could take place (Buzhdygan et al. 2020; DeOre et al. 2021; Motta et al. 2023; Rodriguez-Morales et al. 2022; Suprewicz et al. 2022; Torices et al. 2021; Yang et al. 2022). In contrast, other studies have shown that inoculation of BMECs with SARS-CoV-2 or spike protein only does not affect the expression or the arrangement of tight junction proteins (Constant et al. 2021; Krasemann et al. 2022; Zhang et al. 2021). We observed maximal TEER values of 80–100 $\Omega.cm^2$ in our multi-culture BBB model. While this is lower than TEER values in vivo, a study by Stone et al. 2019 (Stone et al. 2019), on which our model was based, observed that 45 $\Omega.cm^2$ was an appropriate TEER value to ensure barrier integrity. A review by Helms et al. 2016; reported the wide variations in TEER values observed in in vitro BBB models, which likely reflect differences in experimental setup, operator variation and cell types used. Of note, in that review, reported TEER values for human BBB models also varied with TEER values of 30–60 $\Omega.cm^2$ reported (Helms et al. 2016).

Pro-inflammatory cytokines such as IL-1β and TNF-α are known to disrupt tight junctions and, consequently, the integrity of the BBB (Yang et al. 2022). Our study demonstrates that exposure to SARS-CoV-2 promotes endothelial activation and hyper-inflammatory responses when virus is inoculated on either the luminal or the abluminal side of the BBB models. All of the cells in our BBB model, including BMECs, astrocytes, pericytes, and microglia, were activated by SARS-CoV-2 or spike protein. The gene expression of pro-inflammatory cytokines, such as Il-1β and immune cell chemoattractants including CXCL-10 and CCL-2, were significantly upregulated by inoculation with inactivated SARS-CoV-2 or spike protein. We also observed a significant increase in the gene expression of adhesion molecules such as ICAM1, proteinases, and cell death mediators. Our results are consistent with previous reports showing that inoculation with SARS-CoV-2 or viral spike protein induces high levels of inflammatory response in BMEC cultures (Buzhdygan et al. 2020; Krasemann et al. 2022; Motta et al. 2023; Suprewicz et al. 2022; Yang et al. 2022) and spike protein can activate the NLRP3 inflammasome in microglia (Albornoz et al. 2023). Furthermore, cytokines can stimulate the expression of several adhesion molecules on BMEC to facilitate activated leukocyte entry into the CNS leading to BBB disruption (Dietrich 2002) and the exacerbation of neuroinflammation initiated by viral infection. Of note, several studies have demonstrated that disruption of the BBB is related to the onset and progression of various neurological and cerebrovascular diseases, including stroke, traumatic brain injury, brain tumor, multiple sclerosis, Alzheimer's and Parkinson's disease, epilepsy, edema, glaucoma, and amyotrophic lateral sclerosis (Archie et al. 2021) which may explain the CNS disorders observed among acute and post-acute COVID-19 patients.

This study has several limitations. To exclude the possibility of host cell derived factors from infected VeroE6 cells causing perturbations in tight junction expression, we chose to evaluate the effect of recombinant SARS-CoV-2 spike protein only on tight junction expression, and observed tight junction alterations following spike treatment that could not be attributed to non-specific effects from infected VeroE6 supernatants. In contrast, we opted to evaluate heat inactivated SARS-CoV-2 and mock supernatants from VeroE6 cells in addition to TNF-α and IFN-g treatment as a positive control, with the caveat that it is possible that non-specific factors produced by infected VeroE6 cells may have activated some inflammatory pathways in the gene expression assay. However, to control for this, we heat-inactivated supernatants from both infected and mock VeroE6 cultures which could be expected to inactivate or lower the activity of inflammatory mediators (Labossiere et al. 2024). We also compared the ability of both spike treatment and heat inactivated SARS-CoV-2 to stimulate cytokine and chemokines at the protein level using ELISA, which provides a direct comparison of both stimuli concurrently. We did not evaluate endothelial damage directly or the effects of SARS-CoV-2 on the coagulation cascade which has been reported. We initially assessed a range of spike protein concentrations for their ability to disrupt BBB tight junctions and barrier integrity in our model and the spike protein concentrations used were based on the reproducible effects observed with concentrations from 0.5 to 5 µg. This concentration range is higher than circulating spike antigen levels reported in vivo, but it is consistent with other studies using in vitro models such as the study investigating SARS-CoV-2 spike effects on brain endothelium and SARS-CoV-2 spike stimulation of peripheral endothelial cells in vitro by Cano-Mendez et al. 2026 (Cano-Mendez et al. 2026).

It is also possible that spike protein concentrations in the CNS may differ from circulating spike levels as detectable levels have been shown to persist in the brain of humans and mice (Rong et al. 2024). We evaluated the response of cells of the BBB to exposure of inactivated SARS-CoV-2 or spike protein to both luminal and abluminal compartments of the BBB model to model exposure from the blood or brain side of the BBB, respectively. It is possible that diffusion of spike protein or inactivated virus across the BBB models occurred which may not have limited cellular responses exclusively to the luminal or abluminal compartments. However, it is possible that SARS-CoV-2 or spike also crosses the BBB in vivo and that cellular responses are similar to those modelled in vitro in the present study.

In conclusion, the present study demonstrates that SARS-CoV-2 compromises the integrity of a human in vitro BBB model in the absence of viral infection of BBB-forming cells. SARS-CoV-2 neuroinflammation may result from exposure of the BBB to viral proteins in the absence of infection, and this can occur from exposure to either the blood, luminal, side of the BBB model, or the brain, abluminal, side, potentially following microglial activation and cytokine or chemokine release. Importantly, neuropathology in COVID-19 patients may be driven by a combination of both direct infection and virus-driven immunopathology. Therefore, this study adds to the body of data on SARS-CoV-2 neurological disease and directly complements and builds upon our previous study which specifically investigated the neurotropism of SARS-CoV-2 (Haverty et al. 2024). The present study highlights that BBB disruption does not need to occur following direct SARS-CoV-2 infection, and the role of the peripheral and central immune responses to SARS-CoV-2 may play a key role in neuropathology in COVID-19 patients.

Acknowledgements The authors acknowledge the University College Dublin Veterinary Medicine Biosafety Level 3 Laboratory for facilitating experiments with SARS-CoV-2. This study was funded by Research Ireland award 20/COV/8492.

Author contributions All authors contributed to the study conception and design. Material preparation, data collection and analysis were performed by Habib Jmii, Ruth Haverty, Keith Rochfort and Nicola Fletcher. The first draft of the manuscript was written by Habib Jmii and all authors commented on previous versions of the manuscript. All authors read and approved the final manuscript.

Data availability All data supporting the findings of this study are available within the paper and its Supplementary Information. Primer sequences used for PCR experiments are provided in Table 1.

Declarations

Competing interests The authors declare no competing interests.

References

Alajangi HK, Kaur M, Sharma A, Rana S, Thakur S, Chatterjee M, Singla N, Jaiswal PK, Singh G, Barnwal RP (2022) Blood-brain barrier: emerging trends on transport models and new-age strategies for therapeutics intervention against neurological disorders. Mol Brain 15:49

Albornoz EA, Amarilla AA, Modhiran N, Parker S, Li XX, Wijesundara DK, Aguado J, Zamora AP, McMillan CLD, Liang B, Peng NYG, Sng JDJ, Saima FT, Fung JN, Lee JD, Paramitha D, Parry R, Avumegah MS, Isaacs A, Lo MW, Miranda-Chacon Z, Bradshaw D, Salinas-Rebolledo C, Rajapakse NW, Wolvetang EJ, Munro TP, Rojas-Fernandez A, Young PR, Stacey KJ, Khromykh AA, Chappell KJ, Watterson D, Woodruff TM (2023) SARS-CoV-2 drives NLRP3 inflammasome activation in human microglia through spike protein. Mol Psychiatry 28:2878–2893

Aragao M, Leal MC, Cartaxo Filho OQ, Fonseca TM, Valenca MM (2020) Anosmia in COVID-19 Associated with Injury to the Olfactory Bulbs Evident on MRI. AJNR Am J Neuroradiol 41:1703–1706

Archie SR, Al Shoyaib A, Cucullo L (2021) Blood-Brain Barrier Dysfunction in CNS Disorders and Putative Therapeutic Targets: An Overview. Pharmaceutics 13

Briguglio M, Bona A, Porta M, Dell'Osso B, Pregliasco FE, Banfi G (2020) Disentangling the Hypothesis of Host Dysosmia and SARS-CoV-2: The Bait Symptom That Hides Neglected Neurophysiological Routes. Front Physiol 11:671

Buzhdygan TP, DeOre BJ, Baldwin-Leclair A, Bullock TA, McGary HM, Khan JA, Razmpour R, Hale JF, Galie PA, Potula R, Andrews AM, Ramirez SH (2020) The SARS-CoV-2 spike protein alters barrier function in 2D static and 3D microfluidic in-vitro models of the human blood-brain barrier. Neurobiol Dis 146:105131

Cano-Mendez A, Garcia-Larragoiti N, Ambriz-Murillo Y, Velez-Chavez J, Vega-Agavo R, Vazquez-Marrufo G, Higareda-Mendoza AE, Ochoa-Zarzosa A, Viveros-Sandoval ME (2026) Endothelial Cell Activation by SARS-CoV-2 Spike Protein and Its RBD: Central Player of the Immunothrobotic Response in COVID-19. Curr Issues Mol Biol 48(2):161

Cappelletti G, Brambilla L, Strizzi S, Limanaqi F, Melzi V, Rizzuti M, Nizzardo M, Saulle I, Trabattoni D, Corti S, Clerici M, Biasin M (2025) iPSC-derived human cortical organoids display profound alterations of cellular homeostasis following SARS-CoV-2 infection and Spike protein exposure. FASEB J 39:e70396

Cavallieri F, Fioravanti V, Bove F, Del Prete E, Meoni S, Grisanti S, Zedde M, Pascarella R, Moro E, Valzania F (2022) COVID-19 and Parkinsonism: A Critical Appraisal. Biomolecules 12

Chomczynski P, Sacchi N (2006) The single-step method of RNA isolation by acid guanidinium thiocyanate-phenol-chloroform extraction: twenty-something years on. Nat Protoc 1:581–585

Constant O, Barthelemy J, Bollore K, Tuaillon E, Gosselet F, Chable-Bessia C, Merida P, Muriaux D, Van de Perre P, Salinas S, Simonin Y (2021) SARS-CoV-2 Poorly Replicates in Cells of the Human Blood-Brain Barrier Without Associated Deleterious Effects. Front Immunol 12:697329

Crunfli F, Carregari VC, Veras FP, Silva LS, Nogueira MH, Antunes A, Vendramini PH, Valenca AGF, Brandao-Teles C, Zuccoli GDS, Reis-de-Oliveira G, Silva-Costa LC, Saia-Cereda VM, Smith BJ, Codo AC, de Souza GF, Muraro SP, Parise PL, Toledo-Teixeira DA, Santos de Castro IM, Melo BM, Almeida GM, Firmino EMS, Paiva IM, Silva BMS, Guimaraes RM, Mendes ND, Ludwig RL, Ruiz GP, Knittel TL, Davanzo GG, Gerhardt JA, Rodrigues PB, Forato J, Amorim MR, Brunetti NS, Martini MC, Benatti MN, Batah SS, Siyuan L, Joao RB, Aventurato IK, Rabelo de Brito M, Mendes MJ, da Costa BA, Alvim MKM, da Silva Junior JR, Damiao LL, de Sousa IMP, da Rocha ED, Goncalves SM, Lopes da Silva LH, Bettini V, Campos BM, Ludwig G, Tavares LA, Pontelli MC, Viana RMM, Martins RB, Vieira AS, Alves-Filho JC, Arruda E, Podolsky-Gondim GG, Santos MV, Neder L, Damasio A, Rehen S, Vinolo MAR, Munhoz CD, Louzada-Junior P, Oliveira RD, Cunha FQ, Nakaya HI, Mauad T, Duarte-Neto AN, Ferraz da, Silva LF, Dolhnikoff M, Saldiva PHN, Farias AS, Cendes F, Moraes-Vieira PMM, Fabro AT, Sebollela A, Proenca-Modena JL, Yasuda CL, Mori MA, Cunha TM, Martins-de-Souza D (2022) Morphological, cellular, and molecular basis of brain infection in COVID-19 patients. Proc Natl Acad Sci U S A 119: e2200960119

de Maistre E, Savard P, Guinot PG (2023) COVID-19 and the Concept of Thrombo-Inflammation: Review of the Relationship between Immune Response, Endothelium and Coagulation. J Clin Med 12(23):7425

DeOre BJ, Tran KA, Andrews AM, Ramirez SH, Galie PA (2021) SARS-CoV-2 Spike Protein Disrupts Blood-Brain Barrier Integrity via RhoA Activation. J Neuroimmune Pharmacol 16:722–728

Dietrich JB (2002) The adhesion molecule ICAM-1 and its regulation in relation with the blood-brain barrier. J Neuroimmunol 128:58–68

Ermis U, Rust MI, Bungenberg J, Costa A, Dreher M, Balfanz P, Marx G, Wiesmann M, Reetz K, Tauber SC, Schulz JB (2021) Neurological symptoms in COVID-19: a cross-sectional monocentric study of hospitalized patients. Neurol Res Pract 3:17

Fuchs V, Kutza M, Wischnewski S, Deigendesch N, Lutz L, Kulsvehagen L, Ricken G, Kappos L, Tzankov A, Hametner S, Frank S, Schirmer L, Probstel AK (2021) Presence of SARS-CoV-2 Transcripts in the Choroid Plexus of MS and Non-MS Patients With COVID-19. Neurol Neuroimmunol Neuroinflamm 8(2):e957

Guinan AF, Rochfort KD, Fitzpatrick PA, Walsh TG, Pierotti AR, Phelan S, Murphy RP, Cummins PM (2013) Shear stress is a positive regulator of thimet oligopeptidase (EC3.4.24.15) in vascular endothelial cells: consequences for MHC1 levels. Cardiovasc Res 99:545–554

Haidar MA, Shakkour Z, Reslan MA, Al-Haj N, Chamoun P, Habashy K, Kaafarani H, Shahjouei S, Farran SH, Shaito A, Saba ES, Badran B, Sabra M, Kobeissy F, Bizri M (2022) SARS-CoV-2 involvement in central nervous system tissue damage. Neural Regen Res 17:1228–1239

Harati R, Hammad S, Tlili A, Mahfood M, Mabondzo A, Hamoudi R (2022) miR-27a-3p regulates expression of intercellular junctions at the brain endothelium and controls the endothelial barrier permeability. PLoS ONE 17:e0262152

Haverty R, McCormack J, Evans C, Purves K, O'Reilly S, Gautier V, Rochfort K, Fabre A, Fletcher NF (2024) SARS-CoV-2 infects neurons, astrocytes, choroid plexus epithelial cells and pericytes of the human central nervous system in vitro. J Gen Virol 105(7):002009

Helms HC, Abbott NJ, Burek M, Cecchelli R, Couraud PO, Deli MA, Forster C, Galla HJ, Romero IA, Shusta EV, Stebbins MJ, Vandenhaute E, Weksler B, Brodin B (2016) In vitro models of the blood-brain barrier: An overview of commonly used brain endothelial cell culture models and guidelines for their use. J Cereb Blood Flow Metab 36:862–890

Helms J, Kremer S, Merdji H, Clere-Jehl R, Schenck M, Kummerlen C, Collange O, Boulay C, Fafi-Kremer S, Ohana M, Anheim M, Meziani F (2020) Neurologic Features in Severe SARS-CoV-2 Infection. N Engl J Med 382:2268–2270

Jagst M, Pottkamper L, Gomer A, Pitarokoili K, Steinmann E (2024) Neuroinvasion and neurotropism of severe acute respiratory syndrome coronavirus 2 infection. Curr Opin Microbiol 79:102474

Krasemann S, Haferkamp U, Pfefferle S, Woo MS, Heinrich F, Schweizer M, Appelt-Menzel A, Cubukova A, Barenberg J, Leu J, Hartmann K, Thies E, Littau JL, Sepulveda-Falla D, Zhang L, Ton K, Liang Y, Matschke J, Ricklefs F, Sauvigny T, Sperhake J, Fitzek A, Gerhartl A, Brachner A, Geiger N, Konig EM, Bodem J, Franzenburg S, Franke A, Moese S, Muller FJ, Geisslinger G, Claussen C, Kannt A, Zaliani A, Gribbon P, Ondruschka B, Neuhaus W, Friese MA, Glatzel M, Pless O (2022) The blood-brain barrier is dysregulated in COVID-19 and serves as a CNS entry route for SARS-CoV-2. Stem Cell Rep 17:307–320

Kumar A, Pareek V, Prasoon P, Faiq MA, Kumar P, Kumari C, Narayan RK (2020) Possible routes of SARS-CoV-2 invasion in brain: In context of neurological symptoms in COVID-19 patients. J Neurosci Res 98:2376–2383

Labossiere EH, Gonzalez-Diaz S, Enns S, Lopez P, Yang X, Kidane B, Vazquez-Grande G, Siddik AB, Kung SK, Sandstrom P, Ravandi A, Ball TB, Su RC (2024) Detectability of cytokine and chemokine using ELISA, following sample-inactivation using Triton X-100 or heat. Sci Rep 14:26777

Mao L, Jin H, Wang M, Hu Y, Chen S, He Q, Chang J, Hong C, Zhou Y, Wang D, Miao X, Li Y, Hu B (2020) Neurologic Manifestations of Hospitalized Patients With Coronavirus Disease 2019 in Wuhan, China. JAMA Neurol 77:683–690

Megha KB, Joseph X, Akhil V, Mohanan PV (2021) Cascade of immune mechanism and consequences of inflammatory disorders. Phytomedicine 91:153712

Meinhardt J, Radke J, Dittmayer C, Franz J, Thomas C, Mothes R, Laue M, Schneider J, Brunink S, Greuel S, Lehmann M, Hassan O, Aschman T, Schumann E, Chua RL, Conrad C, Eils R, Stenzel W, Windgassen M, Rossler L, Goebel HH, Gelderblom HR, Martin H, Nitsche A, Schulz-Schaeffer WJ, Hakroush S, Winkler MS, Tampe B, Scheibe F, Kortvelyessy P, Reinhold D, Siegmund B, Kuhl AA, Elezkurtaj S, Horst D, Oesterhelweg L, Tsokos M, Ingold-Heppner B, Stadelmann C, Drosten C, Corman VM, Radbruch H, Heppner FL (2021) Olfactory transmucosal SARS-CoV-2 invasion as a port of central nervous system entry in individuals with COVID-19. Nat Neurosci 24:168–175

Motta CS, Torices S, da Rosa BG, Marcos AC, Alvarez-Rosa L, Siqueira M, Moreno-Rodriguez T, Matos AD, Caetano BC, Martins JSD, Gladulich L, Loiola E, Bagshaw ORM, Stuart JA, Siqueira MM, Stipursky J, Toborek M, Adesse D (2023) Human Brain Microvascular Endothelial Cells Exposure to SARS-CoV-2 Leads to Inflammatory Activation through NF-κB Non-Canonical Pathway and Mitochondrial Remodeling. Viruses-Basel 15(3):745

Naranjo O, Osborne O, Torices S, Toborek M (2022) Vivo Targeting of the Neurovascular Unit: Challenges and Advancements. Cell Mol Neurobiol 42:2131–2146

Nascimento Conde J, Schutt WR, Gorbunova EE, Mackow ER (2020) Recombinant ACE2 Expression Is Required for SARS-CoV-2 To Infect Primary Human Endothelial Cells and Induce Inflammatory and Procoagulative Responses. mBio 11

Nuzzo D, Vasto S, Scalisi L, Cottone S, Cambula G, Rizzo M, Giacomazza D, Picone P (2021) Post-Acute COVID-19 Neurological Syndrome: A New Medical Challenge. J Clin Med 10(9):1947

Osborne O, Peyravian N, Nair M, Daunert S, Toborek M (2020) The Paradox of HIV Blood-Brain Barrier Penetrance and Antiretroviral Drug Delivery Deficiencies. Trends Neurosci 43:695–708

Pang Z, Tang A, He Y, Fan J, Yang Q, Tong Y, Fan H (2024) Neurological complications caused by SARS-CoV-2. Clin Microbiol Rev 37:e0013124

Pellegrini L, Albecka A, Mallery DL, Kellner MJ, Paul D, Carter AP, James LC, Lancaster MA (2020) SARS-CoV-2 Infects the Brain Choroid Plexus and Disrupts the Blood-CSF Barrier in Human Brain Organoids. Cell Stem Cell 27:951–961 e5

Pong S, Karmacharya R, Sofman M, Bishop JR, Lizano P (2020) The Role of Brain Microvascular Endothelial Cell and Blood-Brain Barrier Dysfunction in Schizophrenia. Complex Psychiatry 6:30–46

Popa E, Popa AE, Poroch M, Poroch V, Ungureanu MI, Slanina AM, Bacusca A, Coman EA (2025) The Molecular Mechanisms of Cognitive Dysfunction in Long COVID: A Narrative Review. Int J Mol Sci 26(11):5102

Proust A, Queval CJ, Harvey R, Adams L, Bennett M, Wilkinson RJ (2023) Differential effects of SARS-CoV-2 variants on central nervous system cells and blood-brain barrier functions. J Neuroinflammation 20:184

Ramani A, Muller L, Ostermann PN, Gabriel E, Abida-Islam P, Muller-Schiffmann A, Mariappan A, Goureau O, Gruell H, Walker A, Andree M, Hauka S, Houwaart T, Dilthey A, Wohlgemuth K, Omran H, Klein F, Wieczorek D, Adams O, Timm J, Korth C, Schaal H, Gopalakrishnan J (2020) SARS-CoV-2 targets neurons of 3D human brain organoids. EMBO J 39:e106230

Reiken S, Sittenfeld L, Dridi H, Liu Y, Liu X, Marks AR (2022) Alzheimer's-like signaling in brains of COVID-19 patients. Alzheimers Dement 18:955–965

Rhea EM, Banks WA (2019) Role of the Blood-Brain Barrier in Central Nervous System Insulin Resistance. Front Neurosci 13:521

Rodriguez-Morales J, Guartazaca-Guerrero S, Rizo-Tellez SA, Viurcos-Sanabria R, Barron EV, Hernandez-Valencia AF, Nava P, Escobedo G, Carrillo-Ruiz JD, Mendez-Garcia LA (2022) Blood-brain Barrier Damage is Pivotal for SARS-CoV-2 Infection to the Central Nervous System. Exp Neurobiol 31:270–276

Roe K, Kumar M, Lum S, Orillo B, Nerurkar VR, Verma S (2012) West Nile virus-induced disruption of the blood-brain barrier in mice is characterized by the degradation of the junctional complex proteins and increase in multiple matrix metalloproteinases. J Gen Virol 93:1193–1203

Roe K, Orillo B, Verma S (2014) West Nile virus-induced cell adhesion molecules on human brain microvascular endothelial cells regulate leukocyte adhesion and modulate permeability of the in vitro blood-brain barrier model. PLoS ONE 9:e102598

Rong Z, Mai H, Ebert G, Kapoor S, Puelles VG, Czogalla J, Hu S, Su J, Prtvar D, Singh I, Schadler J, Delbridge C, Steinke H, Frenzel H, Schmidt K, Braun C, Bruch G, Ruf V, Ali M, Suhs KW, Nemati M, Hopfner F, Ulukaya S, Jeridi D, Mistretta D, Caliskan OS, Wettengel JM, Cherif F, Kolabas ZI, Molbay M, Horvath I, Zhao S, Krahmer N, Yildirim AO, Ussar S, Herms J, Huber TB, Tahirovic S, Schwarzmaier SM, Plesnila N, Hoglinger G, Ondruschka B, Bechmann I, Protzer U, Elsner M, Bhatia HS, Hellal F, Erturk A (2024) Persistence of spike protein at the skull-meninges-brain axis may contribute to the neurological sequelae of COVID-19. Cell Host Microbe 32:2112–2130e10

Rubin LH, Shi W, Azola A, Bhattacharyya A, Dastgheyb RM, Wu J, Penna CD, Parker H, Santiuste I, Ehrenspeck A, Coughlin JM, Vannorsdall TD, Lu H, Veenhuis R (2025) Blood-Brain barrier disruption in long COVID and cognitive correlates: A cross-sectional MRI study. Brain Behav Immun 129:989–999

Samudyata, Oliveira AO, Malwade S, Rufino de Sousa N, Goparaju SK, Gracias J, Orhan F, Steponaviciute L, Schalling M, Sheridan SD, Perlis RH, Rothfuchs AG, Sellgren CM (2022) SARS-CoV-2 promotes microglial synapse elimination in human brain organoids. Mol Psychiatry 27:3939–3950

Sia SF, Yan LM, Chin AWH, Fung K, Choy KT, Wong AYL, Kaewpreedee P, Perera R, Poon LLM, Nicholls JM, Peiris M, Yen HL (2020) Pathogenesis and transmission of SARS-CoV-2 in golden hamsters. Nature 583:834–838

Song E, Zhang C, Israelow B, Lu-Culligan A, Prado AV, Skriabine S, Lu P, Weizman OE, Liu F, Dai Y, Szigeti-Buck K, Yasumoto Y, Wang G, Castaldi C, Heltke J, Ng E, Wheeler J, Alfajaro MM, Levavasseur E, Fontes B, Ravindra NG, Van Dijk D, Mane S, Gunel M, Ring A, Kazmi SAJ, Zhang K, Wilen CB, Horvath TL, Plu I, Haik S, Thomas JL, Louvi A, Farhadian SF, Huttner A, Seilhean D, Renier N, Bilguvar K, Iwasaki A (2021) Neuroinvasion of SARS-CoV-2 in human and mouse brain. J Exp Med 218(3):e20202135

Stone NL, England TJ, O'Sullivan SE (2019) A Novel Transwell Blood Brain Barrier Model Using Primary Human Cells. Front Cell Neurosci 13:230

Suprewicz L, Tran KA, Piktel E, Fiedoruk K, Janmey PA, Galie PA, Bucki R (2022) Recombinant human plasma gelsolin reverses increased permeability of the blood-brain barrier induced by the spike protein of the SARS-CoV-2 virus. J Neuroinflammation 19:282

Takata F, Nakagawa S, Matsumoto J, Dohgu S (2021) Blood-Brain Barrier Dysfunction Amplifies the Development of Neuroinflammation: Understanding of Cellular Events in Brain Microvascular Endothelial Cells for Prevention and Treatment of BBB Dysfunction. Front Cell Neurosci 15:661838

Torices S, Cabrera R, Stangis M, Naranjo O, Fattakhov N, Teglas T, Adesse D, Toborek M (2021) Expression of SARS-CoV-2-related receptors in cells of the neurovascular unit: implications for HIV-1 infection. J Neuroinflammation 18:167

Wang HY, Li XL, Yan ZR, Sun XP, Han J, Zhang BW (2020) Potential neurological symptoms of COVID-19. Ther Adv Neurol Disord 13:1756286420917830

Wenzel J, Lampe J, Muller-Fielitz H, Schuster R, Zille M, Muller K, Krohn M, Korbelin J, Zhang L, Ozorhan U, Neve V, Wagner JUG, Bojkova D, Shumliakivska M, Jiang Y, Fahnrich A, Ott F, Sencio V, Robil C, Pfefferle S, Sauve F, Coelho CFF, Franz J, Spiecker F, Lembrich B, Binder S, Feller N, Konig P, Busch H, Collin L, Villasenor R, Johren O, Altmeppen HC, Pasparakis M, Dimmeler S, Cinatl J, Puschel K, Zelic M, Ofengeim D, Stadelmann C, Trottein F, Nogueiras R, Hilgenfeld R, Glatzel M, Prevot V, Schwaninger M (2021) The SARS-CoV-2 main protease M(pro) causes microvascular brain pathology by cleaving NEMO in brain endothelial cells. Nat Neurosci 24:1522–1533

Yang AC, Kern F, Losada PM, Agam MR, Maat CA, Schmartz GP, Fehlmann T, Stein JA, Schaum N, Lee DP, Calcuttawala K, Vest RT, Berdnik D, Lu N, Hahn O, Gate D, McNerney MW, Channappa D, Cobos I, Ludwig N, Schulz-Schaeffer WJ, Keller A, Wyss-Coray T (2021) Dysregulation of brain and choroid plexus cell types in severe COVID-19. Nature 595:565–571

Yang RC, Huang K, Zhang HP, Li L, Zhang YF, Tan C, Chen HC, Jin ML, Wang XR (2022) SARS-CoV-2 productively infects human brain microvascular endothelial cells. J Neuroinflammation 19:149

Zhang L, Zhou L, Bao L, Liu J, Zhu H, Lv Q, Liu R, Chen W, Tong W, Wei Q, Xu Y, Deng W, Gao H, Xue J, Song Z, Yu P, Han Y, Zhang Y, Sun X, Yu X, Qin C (2021) SARS-CoV-2 crosses the blood-brain barrier accompanied with basement membrane disruption without tight junctions alteration. Signal Transduct Target Ther 6:337